Journal of Atmospheric and Solar-Terrestrial Physics 65 (2003) 1337 – 1347

Journal of
ATMOSPHERIC AND
SOLAR-TERRESTRIAL
PHYSICS

www.elsevier.com/locate/jastp

Main phenomenological features of ionospheric precursors of strong earthquakes

S.A. Pulinets[a,b,*], A.D. Legen'ka[b], T.V. Gaivoronskaya[b], V.Kh. Depuev[b]

[a] *Instituto de Geofísica, UNAM, Ciudad Universitaria, Delegación de Coyoacán, 04510, México D.F., Mexico*
[b] *Institute of Terrestrial Magnetism, Ionosphere and Radiowave Propagation, Russian Academy of Sciences (IZMIRAN), Troitsk, 142190 Moscow Region, Russia*

Received 8 August 2001; received in revised form 24 December 2002; accepted 31 July 2003

Abstract

This paper summarizes the results of more than 10 years spent by the authors studying the variations in the ionosphere over seismically active regions several days or hours before strong earthquakes. The physical mechanisms of such variations established by the authors and published previously are submitted in the references. This article is aimed mainly at determining the major characteristic parameters of the observed effects (temporal and spatial variations, range in amplitude, etc.) to provide the means to separate the seismogenic effects from other forms of ionospheric variability. Data obtained by ground-based ionosondes and by topside vertical sounding from satellites are used in conjunction with local probe measurements. The topside vertical profiles of the electron concentration are analyzed. It is shown that the most characteristic effect is that of scale height changes in the vertical distribution of ions and electrons implying a decrease in the mean ion mass within the F-layer due to seismogenic effects. This result is supported by direct mass-spectrometer measurements. Differences between magnetic storm ionospheric disturbances and seismogenic variations within the ionosphere are also discussed.

1. Introduction

Recent publications (Pulinets, 1998a; Liu et al., 2000a; Silina et al., 2001; Chuo et al., 2002) brought out clearly that ionospheric variations do exist associated with the seismic activity and appearing few days or hours before the seismic shocks of large intensity ($M > 5$). The reasons for such kind of ionosphere variability were explained within the frame of global electric circuit conception (Pulinets et al., 1998a, 2000, 2002a). The regional but substantially large-scale changes in atmospheric electricity over seismically active areas before the seismic shock are mapped into the ionosphere by means of a large-scale electric field.

After a period of theoretical and statistical studies the new stage always begins—the practical application of the knowledge gained. Those who want to study the ionospheric variability associated with seismic activity face many difficulties, but the most challenging one is the identification of this kind of variability. More than 10 years spent by the present authors in studying the seismo-ionospheric phenomena led us to classify the main features of ionospheric variations associated with pre-seismic activity. This classification is based on hundreds of cases processed using both ground-based and satellite measurements. It is also based on the knowledge of the ionospheric behavior under both quiet and geomagnetically disturbed conditions as a background for seismo-ionospheric variability separation. For the present study data of ground-based ionosondes and of topside sounding from onboard Alouette-2 and Intercosmos-19 satellites were used together with local plasma measurements onboard the AE-C satellite.

Summarizing, we can state that, the main goal of the present paper is not to discuss neither the physical mechanism, which has been done elsewhere (Pulinets et al., 1998a, 2000, 2002a), nor the statistical confirmation of the observed phenomena (Chen et al., 1999). Instead we collect the main

* Corresponding author. Tel.: +52-55-5622-4139; fax: +52-55-555502486.
E-mail address: pulse@geofisica.unam.mx (S.A. Pulinets).

1364-6826/$ - see front matter
doi:10.1016/j.jastp.2003.07.011

characteristics of ionospheric precursors and place emphasis on those features which permit us to discriminate ionospheric precursors due to seismic activity from other causes of ionospheric variability.

2. When ionosphere starts to feel earthquake preparation

Theoretical calculations (Pulinets et al., 1998a) show that the vertical ground electric field starts to penetrate effectively into the ionosphere and create irregularities in the electron concentration when the area on the ground surface occupied by the anomalous field exceeds 200 km in diameter. This area could be identified with the zone of earthquake preparation (Dobrovolsky et al., 1979) or by determination of the precursory seismic activation zone (Bowman et al., 1998). Here the usual precursors used in seismology are borne in mind, foreshocks, deformations, seismic waves velocity anomalies, etc. Using the Dobrovolsky formula $R = 10^{0.43M}$ where R is the radius of earthquake preparation zone, and M is the earthquake magnitude, for $R = 100$ km, we obtain $M = 4.6$. In the paper of Garavaglia et al. (2000) a good correlation between observed deformations and radon emanations is reported, so that we can identify the size of earthquake preparation zone used in seismology with our scale parameter used for the zone occupied by the anomalous electric field. The changes in radon concentration are due to the deformations and crack formation in the earth's crust, so they should be observed within the zone of earthquake preparation. And in our model we use radon as a source of ionization for the electric field generation mechanism, so we can identify these zones. Using the above estimate we can expect ionosphere reaction from earthquakes with magnitudes larger than 4.6.

Another factor for estimation is the simple scaling. The first-most conducting layer of the ionosphere, E-layer, is at an altitude $\sim$ 100 km, and electric field starts to penetrate into the ionosphere when its spatial scale reaches the size of the height of ionospheric layer. We can say that the quantity between 100 and 200 km is a transition size for the electric field area and correspondent ionosphere reaction, shown in the results of statistical studies (Chen et al., 1999). Ionospheric precursors within 5 days before the seismic shock were registered in 73% of the cases for earthquakes with magnitude 5, and in 100% of the cases for earthquakes with magnitude 6. Therefore we can regard the magnitude 5 as some threshold of ionosphere sensitivity for earthquake preparation.

3. Temporal parameters of ionospheric precursors

With the word 'precursor' in the title of the present paragraph, we would like to underline that it is used for brevity and to indicate that this kind of variation appears before a seismic event. But it does not mean for sure that it could be always used as a real precursor in seismic prediction, in the strict sense of the word used in seismology.

The main source of ionospheric data up to now is the network of ground-based ionosondes. Usually only one ionosonde happens to fall within the area of strong seismic activity such as Chung-Li ionosonde in Taiwan or Rome ionosonde in Central Italy. So we are faced with the case of one-point measurements. When a site within a seismoactive zone is instrumented with only one sensor, the only way to identify seismo-ionospheric variations is through good knowledge of their temporal characteristics. Analysis of ionospheric data from many stations all over the world shows that tentatively the time-dependent evolution can be divided into two parts: one with a time-scale of days and another one with a time-scale of hours. In our mind, this reflects the different parts of the process, days—evolution of the seismic source, hours—combination of electric field and ionosphere variability.

The first question which arises in a temporal characteristics analysis is how early precursors appear prior to a shock, and can be identified. Empirically it was found that precursors appear as early as 5 days before the shock (Pulinets, 1998b). Fig. 1 demonstrates the temporal evolution of the critical frequency deviation ΔfoF2 (color coded) for the longitudinal sector where a series of the earthquakes occurred in Italy. The picture is built by interpolating the ground-based vertical sounding data obtained by a longitudinal chain of European ionospheric stations situated close to 40°N within a longitudinal interval 0°–25°E. The parameters of the earthquakes are given in Table 1. The first two earthquakes occurred at longitude $\sim 14^\circ$, and one can see in the figure that just in this sector the variations differ from variations on other longitudes. Then this anomalous bar shifts a little bit to the East according to the longitude of the third earthquake which is 17°. The resolution is not so good because there are not too many ionosondes in Europe but the tendency of the ionospheric variations is very clear. In other periods where no precursors manifest themselves, the variations are in phase at all stations, which produces the horizontal bars over the entire longitudinal range. The colors reflect the positive and negative variations intrinsic to the ionosphere during different types of disturbances. Let us look more carefully at the anomalous variations near longitude 14°. One can see that the first strong positive deviation within this sector appears 5 days before the shock on 7 of May, i.e. on 2 of May 1984. This visualization procedure was used only to demonstrate that ionospheric precursors really exist. Later it was supported by cross-correlation analysis carried out for two ionosondes situated in such a way that one of the stations was within the seismoactive zone, and the second one having the same geomagnetic latitude was situated on longitude 5–7° to the East or to the West (Gaivoronskaya and Pulinets, 2002). In such a configuration all types of ionospheric variabilities are tracked by both ionosondes synchronously, and the cross-correlation coefficient is very high ($\geqslant 0.9$). It is the

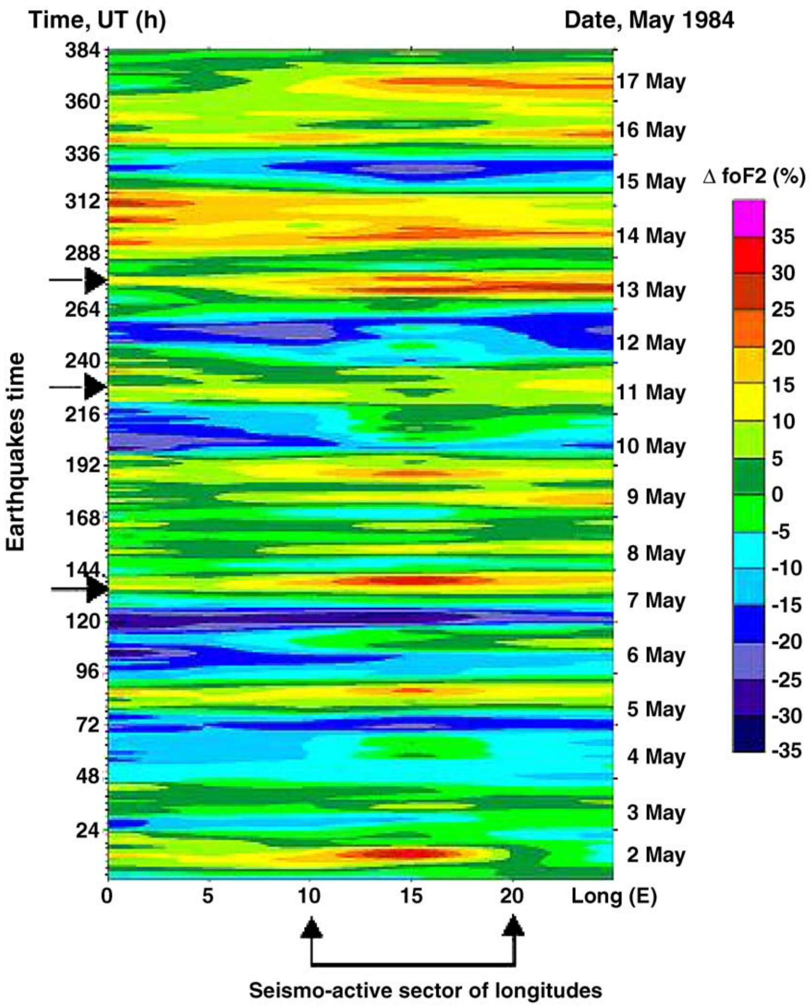

Fig. 1. Deviation of the critical frequency foF2 (color coded) in the longitude sector 0–25°E at latitudes 35–45°N as a function of time for a period of strong seismic activity. Black arrows on the left axis indicate the moments of earthquakes. Left axis—time in hours, right axis—time in days.

same as the horizontal bars in Fig. 1 in the absence of seismic precursors. But before earthquakes, the cross-correlation drops up to values ∼ 0.6 because the far station does not "feel" well the seismo-ionospheric coupling due to limited spatial size of ionospheric region modified by seismic activity. The first minimum of the cross-correlation coefficient is observed usually 5 days before the seismic shock. The same 5 days were obtained for statistical processing of the Taiwanese ionospheric data for 10 years of continuous observations in the seismically active area (Liu et al., 2000b). The ionospheric anomalies associated with the seismic activity were observed 5 days before the seismic shock in Taiwan too. The recently developed technique of the ionospheric precursors registration by GPS TEC observations (Liu et al., 2002) demonstrated the same result. The statistical processing of GPS TEC data for 20 strongest earthquakes ($M \geqslant 6$) from September 1999 to December 2002 in Taiwan area revealed the precursors appearance within the time interval of 1–5 days before the seismic shock (Liu et al., 2004).

If we go to smaller time scales, we see that the ionospheric precursors change as a function of local time. The critical frequency deviation can be positive as well as negative.

Fig. 2a demonstrates the typical appearance of seismic precursors registered at different ionospheric vertical sounding stations for earthquakes with a magnitude from 5.4 up to 7.1 (Pulinets et al., 1998b). Details are given in the figure caption. Because the changes in plasma density associated with the seismic activity are, on an average, of the same order of magnitude as the day-to-day ionospheric variations, the question arises, on how to distinguish seismic

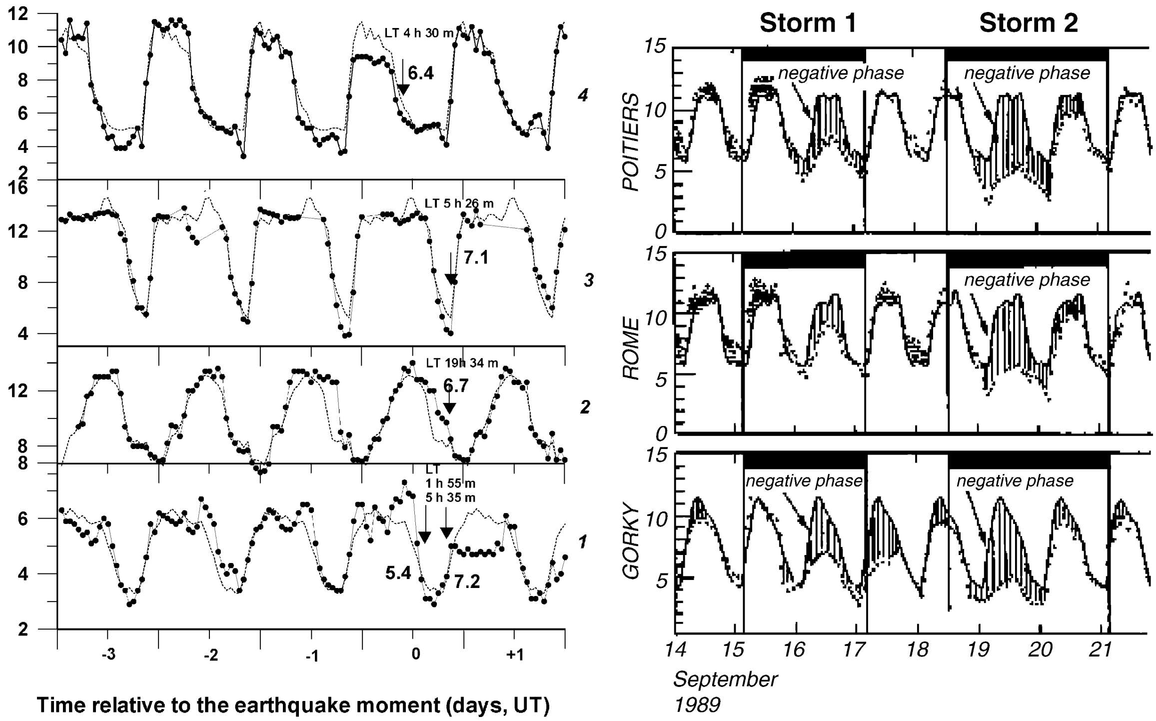

(a) (b)

Fig. 2. (a) Examples of comparison of daily variations foF2 (points) with their monthly median values (dashes), three days before and one day after earthquake, using data of ground-based stations of vertical sounding for various earthquakes: (1) Milkovo (5.09.1971, 18.35 UT, $M = 7,2$,); (2) Rome (23.11.1980, 18.34 UT, $M = 6,7$); (3) Vanimo (16.07.1980, 05.26 UT, $M = 7,3$); (4) Norfolk (14.07.1980, 16.15 UT, $M = 6,6$). Arrows specify the moments of earthquakes. (b) Comparison of daily variations foF2 (points) with the diurnal quiet foF2 (thin solid line) formed by the average of quiet days in September at several European ionospheric stations during two consecutive magnetic storms: Storm 1—Sept. 15–16; Storm 2—Sept. 18–20, 1989.

precursors from the background of daily variations. It was noted early (Pulinets et al., 1998b) that the behavior of the seismo-ionospheric precursors shows some regularity in local time. The first conclusion was that, for specific intervals of local time, the deviation would be either negative or positive. But later studies (Chen et al., 1999) have shown that the situation is more complex. While the behavior in local time has some regularity, it is different for different days prior to the shock. The complex chain of physical processes contributing to its generation could explain such an intricate behavior of the ionospheric precursor. Among the possible sources of variability we have to consider the geological structure of the region of study and especially the structure of the tectonic faults, the source mechanisms for the given earthquakes (slip, thrust, etc.), the sporadity or regularity of the emanations from the ground into the atmosphere, the atmospheric (weather) conditions, regular daily variations of the ionosphere parameters, and the observation point positions in relation to the future epicenter position. The last point is illustrated in Fig. 3. Considering our theoretical calculations the distribution of the electron concentration within the F-region at an altitude of 250 km, we can obtain completely different results for the same distribution in ionosphere depending on the ionosonde position. At position a—epicenter to the north-east from the ionosonde, we have positive deviation, position b—epicenter to the north-west from the ionosonde, we have negative deviation, position c—epicenter to the north from ionosonde, we have almost zero deviation, position d—epicenter to the north-north-west from the ionosonde, we also have negative deviation but much smaller than in position b. This distribution was calculated for a “normal” (directed down) atmospheric field direction, but a change in the electric field direction is often observed before the seismic shocks (Nikiforova and Michnowski, 1995; Vershinin et al., 1999). This means that the sign of the dipole distribution within the ionosphere can reverse, which in turn will reflect on the ionosonde records as a change of the deviation sign. Therefore, we can interpret the different shape of variations observed by ionosondes for different earthquakes as being due to relative positions of the ionosondes and epicenter and to reversals of the atmospheric electric field direction.

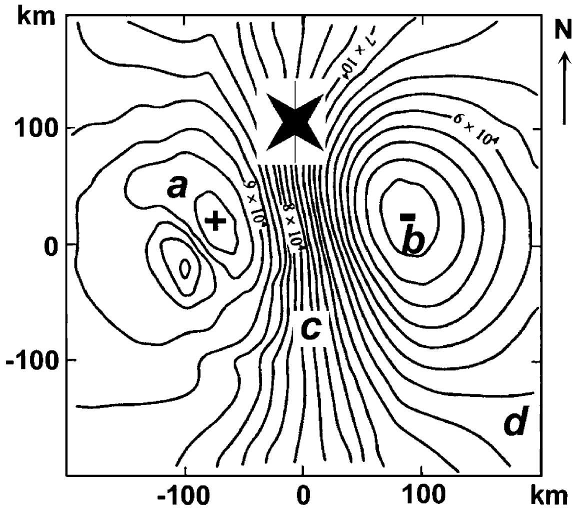

Fig. 3. Model distribution of the electron concentration at the altitude 250 km. Solid dot—the vertical projection of the anomalous electric field source.

Based on our theoretical calculations we can use the following statement as the working hypothesis: *for fixed relative positions of the earthquake source and observation points and for the same source mechanism, the shape of the ionospheric precursor should be the same (or very similar) for recurring earthquakes occurring in the same epicenter region or close to it*. Usually in the vicinity of the ionosonde (within the radius of 500 km) only one active tectonic fault is situated. Therefore one can expect the same ionospheric variations observed before the earthquake at the given point. In order to take into account long-time (days before seismic shock), as well as short-time (within one day—local time) variations it was proposed to construct a three-dimensional portrait of the precursor where one axis (Y) is the local time, the second axis (X) is the number of days prior to the earthquake, and the third coordinate (color) is the amplitude of the deviation of the critical frequency from an undisturbed state. We called this pattern recognition technique a “precursor mask” (Lomonosov et al., 2000; Pulinets et al., 2002b). The mask imposed on the data will help to identify the one-point observation precursors within the flow of data. For estimation, we use the specially designed similarity function S_n where ionospheric data are presented in matrix form. If S_n grows with the number of earthquakes n, it means that ionospheric data matrixes A_{jk} are similar, which permits the selection of a sequence similar to the earthquake precursor shape from the data flow. Taking into account the above discussion one should expect different masks for different locations. Retrospective data of ionospheric measurements should be analyzed for every site in order to obtain the appropriate mask that identifies the seismic precursors. Fig. 4 demonstrates the mask for the ionospheric station at Rome. This mask can be applied to earthquake prediction in Central Italy.

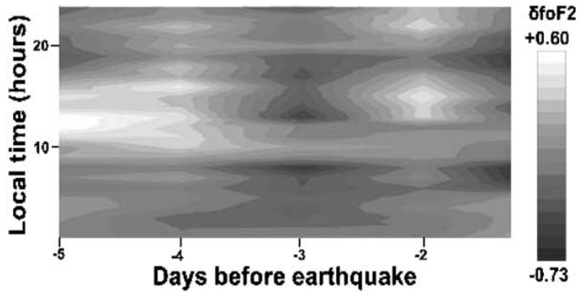

Fig. 4. Temporal mask for pre-seismic ionospheric variations in Italy (Rome ionospheric station) Horizontal axis—days before the earthquake, vertical axis—local time.

The difference between the seismo-ionospheric variations and variations during magnetic storms is clearly seen from their graphic comparison (Fig. 2). In Fig. 2a, where the seismo-ionospheric variations are presented, the deviations of the critical frequency are not so pronounced as during geomagnetic storms (Fig. 2b), and do not last so long. Usually, the duration of the deviation of one sign does not exceed 4–6 h. Only for very strong earthquakes (such as Good Friday earthquake at Alaska, 1964) the duration of the anomalous deviation of the same sign can approach 12 h (Pulinets and Legen’ka, 2003). But for magnetic storms a long duration of the negative phase (more than 12 h) is normal. In Fig. 2b, where data for two consecutive magnetic storms are presented, collected at three midlatitude ionospheric stations, one can observe a very strong negative deviation lasting more than 24 h, and the variations never have an oscillating character (positive to negative reversals during few hours) as one can see in Fig. 2a for the Milkovo station (1). The amplitude variations during a magnetic storm, as one can see from Fig. 2b, are also more pronounced, as much as two- or three-fold. At the same time estimates made in (Pulinets et al., 1998b) on the basis of analysis of ionospheric effects of 54 worldwide earthquakes show ± 30% maximum deviation for ionospheric precursors.

Another very important and maybe decisive factor is that the ionospheric effect of a geomagnetic storm has a global impact. It is observed all over the world while, the seismogenic effect is observed only by stations close to the anticipated epicenter (less than 2000 km). This leads us to the question of the spatial distribution of seismogenic variations within the ionosphere.

4. Spatial distribution of ionospheric precursors

The most appropriate technique to study the spatial distribution of seismo-ionospheric variations is satellite mapping. Measurements of the critical frequency foF2 by vertical sounding from the ground or by topside sounding from satellite give the same values. Therefore, we can use topside sounding for such studies, supplemented by data of ground-based ionospheric stations when they are located within the area mapped by the satellite. The detailed descriptions of the satellite data processing technique and results of the satellite mapping are presented in the paper by Pulinets and Legen'ka (2003). Here we only use the estimated spatial parameters of the ionospheric precursors in the F2 region to supplement the set of their phenomenological characteristics. The topside sounding satellite measurements were made globally, and large-scale ionospheric variations before strong earthquakes were detected at all latitudes. For high-latitude variations the data of the Alouette satellite were used together with ground-based ionosondes to study the effects of the Alaska "Good Friday" earthquake of 1964. For other latitudes the data of the Intercosmos-19 topside sounder were used. Regardless of latitude, the spatial scale of the ionospheric effects for strong earthquakes is the same order of magnitude and is near 20° in longitude as well as in latitude. But one can find the increase of the modified area in the ionosphere with the increase of earthquake magnitude. For all latitudes the satellite data confirm the ground-based data demonstrating the positive and negative variations relative to different local times.

Two new effects were detected by the satellites. Under specific conditions (when both hemispheres are not sunlit) the conjugated effect could be observed. It means that an ionospheric anomaly over a seismically active area is mapped through the geomagnetic field lines on a magnetically conjugated area of opposite hemisphere. An example of such an effect is presented in Fig. 5 for the Irpinia earthquake of 1980 in Central Italy. The second important finding relates to the equatorial ionosphere and is closely related to the conjugated effect described above. In equatorial latitudes the length of the geomagnetic field lines is very short, which facilitates the effect of magnetic conjunction. And it was detected (Pulinets and Legen'ka, 2002) that, if the epicenter falls between the crests of equatorial anomaly, the effect within the ionosphere is observed not only over the epicentral area, but the anomaly also reacts as a whole structure, completely changing its shape and the anomaly magnitude development (crest-to-trough density relation). It appears as though the anomaly crests move towards the geomagnetic equator and disappear before the earthquake in afternoon hours of local time or in contrast, the crests develop in the early morning before sunrise. This implies the existence of the zonal component of the seismically generated electric field after its penetration into the ionosphere and its interaction with the electric field responsible for the fountain effect in the equatorial anomaly. As an independent example of this phenomenon we point to the paper by Liu et al., (2002), where GPS TEC monitoring was used to follow the anomaly modification prior to the last destructive earthquakes in Taiwan.

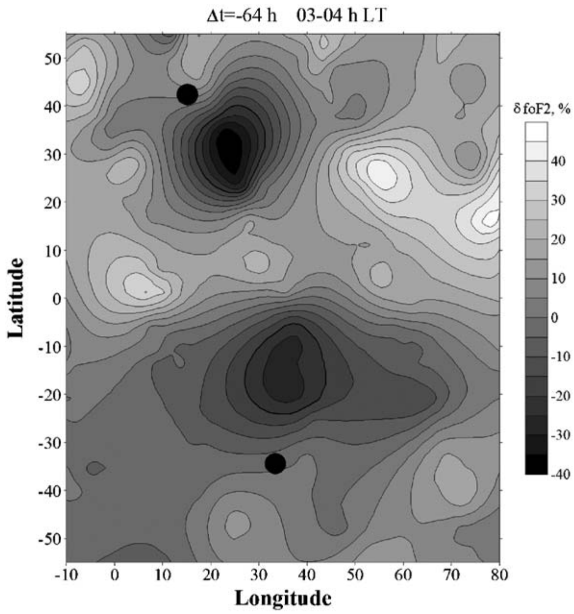

Fig. 5. Critical frequency deviation 2-D distribution using topside and bottomside sounding data registered 40 h before the Irpinia earthquake in Central Italy on 23.11.1980.

5. Pre-seismic variations of the ionospheric plasma parameters

Up to now, in this paper, only the critical frequency variations were described as ionospheric earthquake precursors, but they reflect substantial changes occurring within the whole ionosphere as reflected in variations of the local plasma parameters. To analyze the local plasma parameters variations at different altitudes data from the AE-C local plasma probe were used for the period between January and February 1974 when the orbit of the satellite was elliptical. For the temperature and ion composition measurements we selected times of undisturbed conditions in the absence of magnetic disturbances, periods during magnetic storms, and periods few days before the earthquakes. In the Fig. 6a one can see the effect of a geomagnetic storm on the local temperature parameters in comparison with undisturbed conditions. In Fig. 6b we present a similar comparison, plotting the undisturbed measurements together with those of a satellite pass over a seismically active area before an earthquake. Comparing the figures we note the well-known heating of the ionosphere during the main phase of a magnetic storm when the increase of electron and ion temperatures at middle latitudes can reach 1000 and 2000 K, respectively. But no substantial ionospheric heating was observed neither before nor after the earthquake. Only small (up to 200 K) variations of the electron temperature T_e as well as variations of the temperature of the neutral component T_n are observed prior to earthquakes. These electron temperature

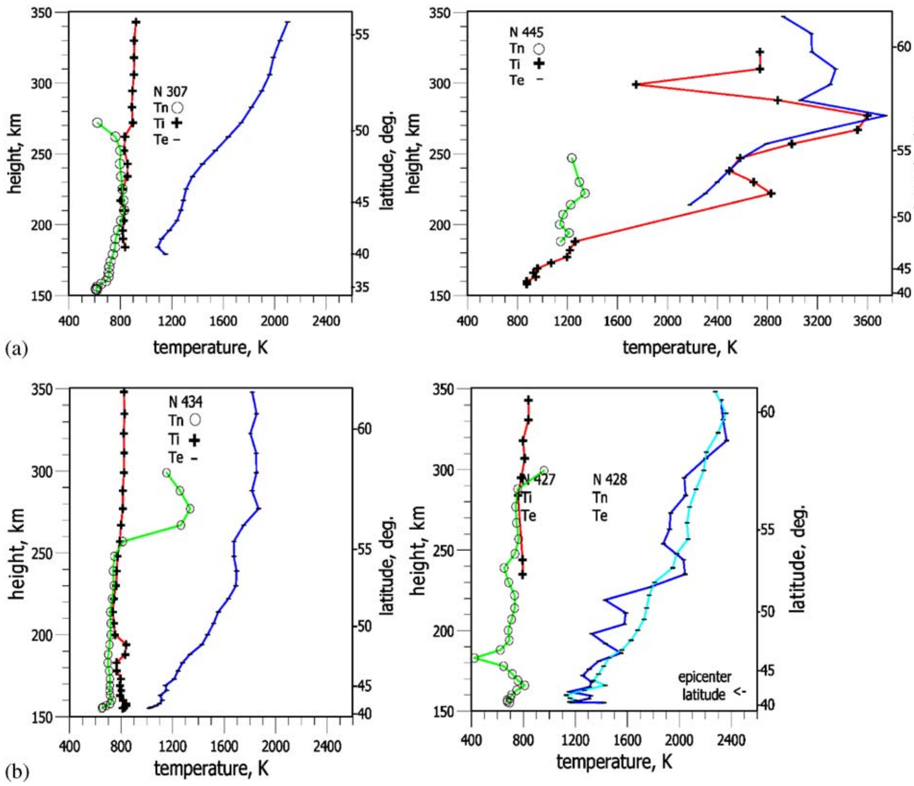

Fig. 6. (a) Examples of temperature profiles measured before (24.01.74) and during the main phase of an ionospheric storm on 25.01.74. Tn, Ti and Te—neutral, ion and electron temperatures, respectively. (b) Measurements during quiet time and several hours before the earthquake, respectively. Earthquake with $M \sim 6.4$ occurred on 24.01.74 at the point 42.1°N, 144.0°E (Hokkaido is 1).

variations before the earthquake exhibit a wave-like character with height—a fact that may imply an acoustic gravity wave propagation effect (Hegai et al., 1997).

Figs. 7a and b represent a similar comparison of effects of a geomagnetic storm and an earthquake but for ion composition. Because even small changes of the ionospheric electric field cause substantial ion drifts, the anomalous electric field appearing within the ionosphere above the region of the impending earthquake plays an important role in the observed variations. Modifications of the concentration of atomic oxygen O^+ at heights of the F2-layer maximum and of the concentration of molecular ions NO^+ and $O2^+$ in the bottom of the layer were observed before earthquakes. It should be noted that the variations of O^+, NO^+ and $O2^+$ concentrations before earthquakes have the same sign (Fig. 7b), contrary to the variations of the ion compositions during the main phase of an ionospheric storm (Fig. 7a), when a decrease of ions O^+ in an F2-layer is accompanied by a substantial increase of concentration of NO^+ and $O2^+$. It is interesting to note that these "in-phase" changes of the ion concentrations before earthquakes are observed regardless of the sign of electron density variations (positive or negative). These peculiarities of the ion composite variations may be used to discriminate between seismically induced variations and geomagnetically disturbed conditions.

The second remarkable feature noticed previously (Bošková et al., 1993) is an increase in the light ion concentration in the ionosphere over the region of impending earthquake activity, implying a decrease in the mean ion mass. This effect is demonstrated in our analysis of the AE-C data and is shown in Fig. 8a where measurements of the mean ion mass are plotted, while the satellite passed over the anticipated earthquake epicenter region one day before the earthquake (dots), and one day after the earthquake (crosses). Measuring simultaneously the electron and ion temperatures and using the formula for the ionosphere height scale (Smith and Kaiser, 1967) the changes in the ionosphere height scale can be obtained:

$$H_s = \frac{T_e + T_i}{M_+/0.85 + (h/R_0 + 1)^2 \mathrm{d}T_e/\mathrm{d}h},$$

where M_+ is mean ion mass, and R_0 is the Earth's radius.

Since there are no noticeable changes in neither the electron nor the ion temperatures during the seismically induced perturbation of the ionosphere, we conclude that the main reason for the height scale changes is due to changes in

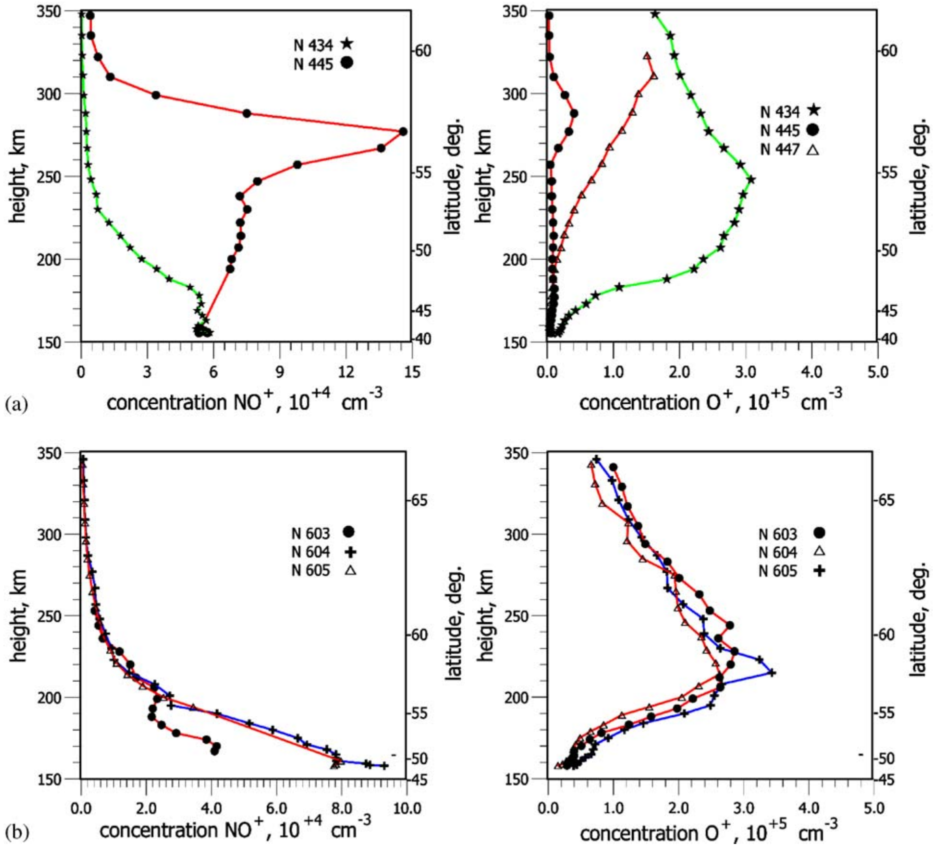

Fig. 7. (a) Variations of NO^+ and O^+ ions, respectively, during the main phase of a magnetic storm (circles) in comparison with quiet conditions (stars). (b) Examples of the variations of NO^+ and O^+ ions prior to an impending earthquake as the satellite passes closest to the epicenter longitude ($< 10^\circ$, points), and far from it ($> 20^\circ$ crosses).

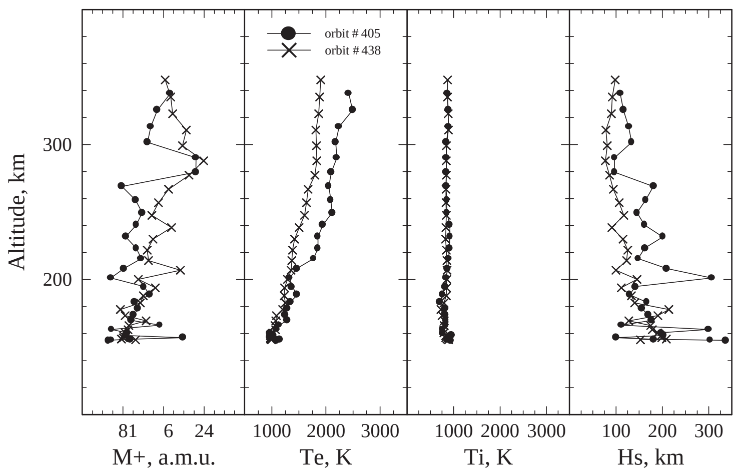

Fig. 8. From left to right AE-C measurements of (a) mean ion mass, (b) electron temperature, (c) ion temperature, (d) calculated height scale of the ionosphere. Crosses—reference level, circles—seismic precursory period.

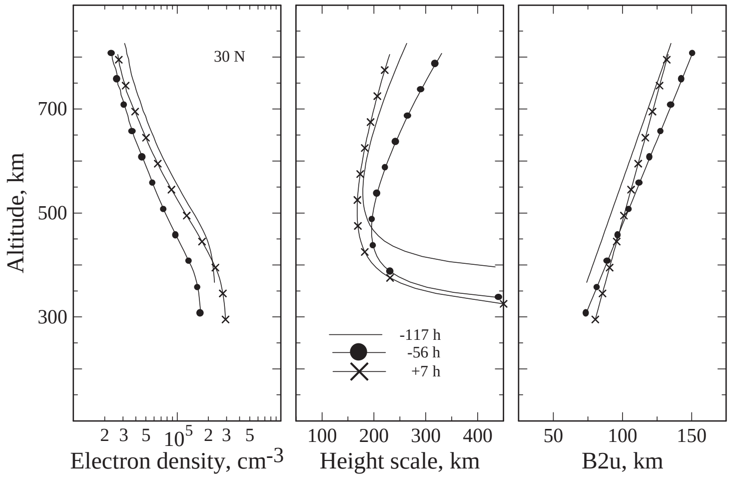

Fig. 9. Topside profiles (left), height scale (middle) and semithickness for the period of the Irpinia earthquake in Southern Italy, November, 1980.

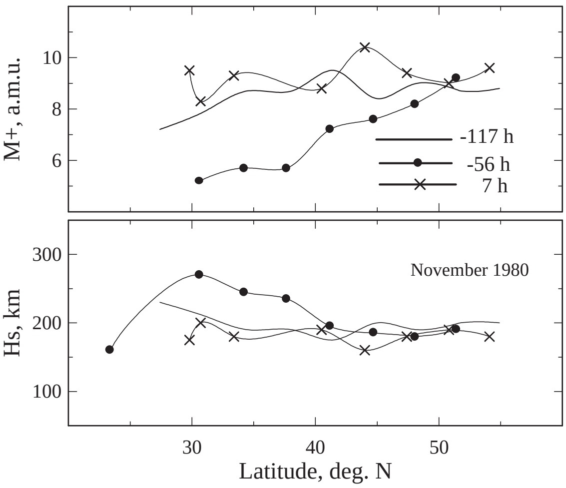

Fig. 10. Mean ion mass (top panel) and height scale (bottom panel) variations over the seismically active region 117 (solid line), 56 (circles) hours before the earthquake and 7 h after it (crosses).

the mean ion mass. Such changes in the height scale can alternatively be obtained by topside sounding i.e. by deriving the height scale from the topside vertical electron profiles. Such measurements were conducted from onboard the Intercosmos-19 satellite and examples of topside profiles for undisturbed conditions and prior to earthquakes are presented in Fig. 9. This figure shows in the left panel the topside profiles measured over the epicenter area 172 and 56 h before the earthquake and 7 h after it, in the middle panel the height scale curves calculated for the given profiles, and in the right panel the semithickness parameter B2u calculated from the model (Depuev and Pulinets, 2001; Nava et al., 2001). These results are presented in Fig. 10. They are consistent with estimates of the mean ion mass derived from the vertical topside electron density profiles, showing an effective decrease in the mean ion mass. This analysis was carried out for the Irpinia earthquake in Italy 23.11.80, 40°46′N, 15°18′E, $M = 6.9$ and corresponds to the critical frequency distribution shown in Fig. 5.

Analysis of in situ measurements of local plasma parameters and topside profiles of the vertical electron concentration distribution reveal the differences in the ionospheric variability during periods of geomagnetic storms and over a seismically active region few days or hours prior to strong earthquakes ($M > 5$). The main differences are:

- An "in-phase" changes of all ion species during seismically induced period effects contrary to those induced by magnetic storms (increase in NO^+ and decrease in O^+ concentrations).
- Decrease of the mean ion mass as the main reason of the scale height variations during seismically induced disturbances but increase in the electron and ion temperatures as the source of the scale height variations during the magnetic storms.

We can conclude that seismically induced ionospheric variability shows unique features that permit us to exploit ionospheric variations before strong earthquakes as a tool for short-term earthquake prediction.

6. Conclusion

In this paper we have tried to demonstrate and pin down the main characteristic features of the seismo-ionospheric variations registered both by ground-based and satellite-borne techniques. These variations involve the spatial and temporal development of the electron density, electron and ion temperatures, ion composition, mean ion mass and vertical distribution of the electron density. Remarkable differences have been identified between the seismo-ionospheric effects and those caused by magnetic storms.

The main characteristics of ionospheric precursors can be enumerated as follows:

- Seismically induced precursors affect the plasma density (relative to a normal non-perturbed state), and are observed between 5 days to a few hours prior to the earthquake.
- The variations (relative to a normal non-perturbed state) can have a positive or negative sign.
- The duration of a seismically induced deviation of a given sign is comparatively short about 4–6 h (relative to magnetic storm effects). Only in cases of very strong earthquakes (such as before the large 1964 Good Friday earthquake, Alaska) can the duration of a seismically induced deviation reach about 12 h.
- The threshold at which seismogenic effects on the ionosphere become observable is determined by the size of the earthquake preparation zone and corresponds to magnitude 5.
- Seismo-ionospheric variations have the same amplitude, on an average, as the day-to-day variability of an ionosphere ($\pm 30\%$), but can be much more pronounced, up to 100%, at particular moments of local time.
- The sign and shape of seismo-ionospheric variations depend on local time. This dependence may be different for different latitudes and longitudes and will require additional research for every geophysical location.
- The affected area of the ionosphere at the height of the F-layer maximum reaches $\sim 40^\circ$ both in latitude and longitude. The size of the area changes with the earthquake magnitude.
- The maximum of the affected area in the ionosphere does not coincide with the vertical projection of the epicenter of the future earthquake.
- The variations in the ionosphere lead to changes in the vertical distribution of the plasma, which leads to an increase in the height scale of the ionosphere.
- The height scale changes are mainly due to changes in the ion mass (increasing concentration of light ions) or due to parallel particle fluxes. They are not due to plasma temperature changes.
- The TEC seismo-ionospheric variations agree well with the measured deviations in the critical frequency.
- Sometimes the corresponding ionospheric effects can be observed in the magnetically conjugated region.

References

Bošková, J., Šmilauer, J., Jiříček, F., Tříska, P., 1993. Is the ion composition of outer ionosphere related to seismic activity. Journal of Atmospheric and Terrestrial Physics 55 (13), 1689–1695.

Bowman, D.D., Ouillon, G., Sammis, C.G., Sornette, A., Sornette, D., 1998. An observation test of the critical earthquake concept. Journal of Geophysical Research 103, 24359–24372.

Chen, Y.I., Chuo, Y.J., Liu, J.Y., Pulinets, S.A., 1999. Statistical study of ionospheric precursors of strong earthquakes at Taiwan area. XXVI URSI General Assembly, Toronto, 13–21 August 1999/Abstracts 745.

Depuev, V.H., Pulinets, S.A., 2001. Epstein function global topside profile modeling on the basis of Intercosmos-19 topside sounding data (quiet conditions), IRI Task Force Activity-2000. Proceedings, Trieste, pp. 35–40.

Dobrovolsky, I.R., Zubkov, S.I., Myachkin, V.I., 1979. Estimation of the size of earthquake preparation zones. Pure and Applied Geophysics 117, 1025–1044.

Gaivoronskaya, T.V., Pulinets, S.A., 2002. Analysis of the F2 layer variability over the areas of seismic activity, Preprint IZMIRAN No. 2(1145), IZMIRAN, Russian Academy of Science, 20pp. Izvestiya, Physics of the Solid Earth, 40 (2004), in press.

Garavaglia, M., Dal Moro, G., Zadro, M., 2000. Radon and tilt measurements in a seismic area: tempreature effects. Physics and Chemistry of the Earth 25 (3), 233–237.

Hegai, V.V., Kim, V.P., Nikiforova, L.I., 1997. A possible mechanism of acoustic-gravity waves in the ionosphere. Journal of Earthquake Predictions Research 6, 584–589.

Liu, J.Y., Chen, Y.I., Pulinets, S.A., Tsai, Y.B., Chuo, Y.J., 2000a. Seismo-ionospheric signatures prior to $M \geqslant 6.0$ Taiwan earthquakes. Geophysical Research Letters 27 (19), 3113–3116.

Liu, J., Chen, Y., Pulinets, S.A., Chuo, Y., 2000b. A statistical study of ionospheric precursors of $M \geqslant 5.0$ earthquakes in Taiwan area. Eos Transactions AGU 81(48), Fall Meeting Supplement, Abstract S11B-07, 2000.

Liu, J.Y., Chuo, Y.J., Pulinets, S.A., Tsai, H.F., Xiaopang Zeng, 2002. A study on the TEC perturbations prior to the Rei-Li, Chi-Chi and Chia-Yi earthquakes. In: Hayakawa, M., Molchanov, O.A. (Eds.), Seismo-Electromagnetics: Lithosphere–Atmosphere–Ionosphere Coupling. TERRAPUB, Tokyo, pp. 297–301.

Liu, J.Y., Chuo, Y.J., Shan, S.J., Tsai, Y.B., Pulinets, S.A., Yu, S.B., 2004. Pre-earthquake-ionospheric anomalies registered by continuous GPS TEC. Annales Geophysicae, submitted for publication.

Lomonosov, A.M., Boyarchuk, K.A., Pulinets, S.A., 2000. New techniques of statistical and spectral analysis of groundbased vertical sounding data to reveal ionospheric precursors. International Workshop on Seismo Electromagnetics of NASDA, September 19–22, Program and Abstracts, University of Electro-Communications, Chofu-City, Tokyo Japan, pp. 155–159.

Nava, B., Radicella, S.M., Pulinets, S., Depuev, V., 2001. Modelling bottom and topside electron density and TEC with profile data from topside ionograms. Advances in Space Research 27 (1), 31–34.

Nikiforova, N.N., Michnowski, S., 1995. Atmospheric electric field anomalies analysis during great Carpatian Earthquakes at Polish Observatory Swider. IUGG XXI General Assembly Abstracts, Boulder, CO, VA11D-16.

Pulinets, S.A., 1998a. Strong earthquakes prediction possibility with the help of topside sounding from satellites. Advances in Space Research 21 (3), 455–458.

Pulinets, S.A., 1998b. Seismic activity as a source of the ionospheric variability. Advances in Space Research 22 (6), 903–906.

Pulinets, S.A., Legen'ka, A.D., 2002. Dynamics of the near-equatorial ionosphere prior to strong earthquakes. Geomagnetism and Aeronomy 42 (2), 227–232.

Pulinets, S.A., Legen'ka, A.D., 2003. Spatial-temporal characteristics of large scale distributions of electron density observed in the ionospheric F-region before strong earthquakes. Cosmic Research 41 (3), 221–229.

Pulinets, S.A., Khegai, V.V., Boyarchuk, K.A., Lomonosov, A.M., 1998a. Atmospheric electric field as a source of ionospheric variability. Physics-Uspekhi 41 (5), 515–522.

Pulinets, S.A., Legen'ka, A.D., Zelenova, T.I., 1998b. Local-time dependence of seismo-ionospheric variations at the F-layer maximum. Geomagnetism and Aeronomy 38 (3), 400–402.

Pulinets, S.A., Boyarchuk, K.A., Hegai, V.V., Kim, V.P., Lomonosov, A.M., 2000. Quasielectrostatic model of atmosphere–thermosphere–ionosphere coupling. Advances in Space Research 26 (8), 1209–1218.

Pulinets, S.A., Boyarchuk, K.A., Hegai, V.V., 2002a. Conception and model of seismo-ionosphere-magnetosphere coupling. In: Hayakawa, M., Molchanov, O.A. (Eds.), Atmospheric and Ionospheric Electromagnetic Phenomena Associated With Earthquakes. TERRAPUB, Tokyo, pp. 353–361.

Pulinets, S.A., Boyarchuk, K.A., Lomonosov, A.M., Khegai, V.V., Liu, J.Y., 2002b. Ionospheric precursors to earthquakes: a preliminary analysis of the $foF2$ critical frequencies at Chung-Li ground-based station for vertical sounding of the ionosphere (Taiwan Island). Geomagnetism and Aeronomy 42 (3), 508–513.

Silina, A.S., Liperovskaya, E.V., Liperovsky, V.A., Meister, C.-V., 2001. Ionospheric phenomena before strong earthquakes. Natural Hazards and Earth System Sciences 1, 113–118.

Smith, P.A., Kaiser, B.A., 1967. Estimates of ionospheric composition and temperature derived from topside sounder electron scale height data. Journal of Atmospheric and Terrestrial Physics 29 (11), 1345–1353.

Vershinin, E.F., Buzevich, A.V., Yumoto, K., Saita, K., Tanaka, Y., 1999. Correlations of seismic activity with electromagnetic emissions and variations in Kamchatka region. In: Hayakawa, M. (Ed.), Atmospheric and Ionospheric Electromagnetic Phenomena Associated with Earthquakes. Terra Scientific Publishing Company, Tokyo, pp. 513–517.